NUMERICAL IMPLEMENTATION IN 1D AND 2D OF A SHAPE OPTIMIZATION PROBLEM WITH ROBIN BOUNDARY CONDITIONS

BENIAMIN BOGOSEL AND MARION FOARE

Abstract. In this paper, we study a shape optimization problem with Robin boundary conditions based on an optimal insulation problem. We prove the Γ-convergence of two approximations towards the functional we want to optimize and we show some numerical experiments in dimension one using finite differences discretization. In dimension two we provide a method of computing the solution of the partial differential equation with Robin boundary condition with the aid of fundamental solutions. This leads to an optimization algorithm on which we observe the behavior of the optimal shape with respect to the geometry and the value of the source.

Keywords: Robin boundary conditions, shape optimization

1. Introduction

In this article we present some aspects related to the numerical study of a shape optimization problem related to thermal insulation. Given a domain $K \subset \mathbb{R}^n$, we consider the pair (Ω, u) such that Ω contains K and $u \equiv g$ on K. We are interested in minimizing the functional

$$F(\Omega, u) = \int_\Omega |\nabla u|^2 dx + \beta \int_{\partial\Omega} u^2 d\sigma + \gamma|\Omega| \tag{1}$$

where the pair (Ω, u) satisfies the constraints stated above and β, γ are fixed positive constants. When Ω is fixed and smooth enough, minimizing $F(\Omega, u)$ amounts to solving the elliptic partial differential equation

$$\begin{cases} \Delta u = 0 & \text{in } \Omega \setminus K \\ \partial_n u + \beta u = 0 & \text{on } \partial\Omega \setminus \partial K \\ u = g & \text{on } \partial K. \end{cases} \tag{2}$$

We note that the case $\beta = 0$ was studied in the classical work of Alt and Caffarelli [AC81]. In order to study the minimizers of (1) the following relaxed formulation in SBV was considered in [BL14]

$$\min_{u \in SBV^{\frac{1}{2}}, u=g \text{ on } K} \int_D |\nabla u|^2 + \beta \int_{J_u} [(u^+)^2 + (u^-)^2] d\sigma + \gamma |\{u > 0\}|. \tag{3}$$

Bucur and Luckhaus [BL14] proved that problem (3) has a solution. Further investigation, and in particular the regularity of the free discontinuity of the jump set, was done by Caffarelli and Kriventsov in [CK16]. In [BG15] Bucur and Giacomini studied shape optimization problems with Robin conditions on the free boundaries.

In [CK16] the authors underline the connection between this problem and an optimal insulating configuration. Indeed, we may assume that there is a heat source given by g on K. We insulate K using Ω and we cover Ω with a thin layer of width ε of highly insulating material (conductivity $1/\varepsilon$). If we also assume that the cost of the insulator per unit of volume is equal to γ then the energy of the configuration has the form

$$\min_{\substack{u \in \mathrm{H}^1_0(\Omega \cup \Sigma_\varepsilon) \\ u=g \text{ on } K}} \int_\Omega |\nabla u|^2 \ \mathrm{dx} + \beta\varepsilon \int_{\Sigma_\varepsilon} |\nabla u|^2 \ \mathrm{dx}.$$

Since $u = 0$ in the complement of $\Omega \cup \Sigma_\varepsilon$, then $|\nabla u| \sim \frac{u}{\varepsilon}$ in Σ_ε. Thus, as ε tends to 0, we obtain (1).

We are interested in finding numerically minimizers of (1). The first approach we use is based on a Γ-convergence relaxation of (3). Indeed, if a sequence F_ε approximates our functional F by Γ-convergence then minimizing F_ε for $\varepsilon \to 0$ we hope to get close to a minimizer of F. We propose two different approximations. The first one is a local approximation using a result of Acerbi and Braides [AB+98]. The second approach is a non-local approximation which works in dimension 1. For both methods we construct numerical algorithms which can successfully approximate solutions to problem (1) in dimension one.

In dimension 2, supposing that Ω is regular enough, we choose to work directly with the PDE formulation (2). This type of problem can be efficiently solved using the method of fundamental solutions. This consists of considering a basis of harmonic functions and searching for solutions u as a linear combination of elements of this basis which satisfy the boundary conditions. For more works concerning the method of fundamental solutions regarding similar problems see [GC99] for aspects regarding Poisson's equation, [Bog16] for Steklov type eigenvalue problems. The case of non-simply connected domains was considered in [AV10]. In this context, the computation of a solution of (2) is fast and precise, and it allows us to construct an algorithm for the shape optimization problem. We are able to test this algorithm in various situations, obtaining precise results in the case where K is a disk and $g \equiv 1$, in accordance with the analytical solution in the radial case. Moreover, computations can be done for general source domain K and source term g. In particular, we are able to verify numerically some questions raised in [CK16] regarding the geometrical properties of the optimal set Ω like convexity or star-shapedness.

Outline. The paper is organized as follows. We provide in Section 2 two Γ-convergence results which provide approximations of the shape optimization functional. In Section 3, we discuss some numerical implementation details and show results of the minimization of the two approximations in dimension one using finite differences discretization. In Section 4 we present a numerical method based on fundamental solutions in order to solve (2) in dimension two. Then we perform some optimization tests for various source domains K and source terms g.

2. Approximations by Γ-convergence

2.1. Local approximation using Acerbi and Braides method.

We construct a first approximation based on the functional proposed by Acerbi and Braides [AB+98, Th. 3.1] :

$$AB_\varepsilon(u,v) = \int_D \psi(v)|\nabla u|^2 \, \mathrm{dx} + \varepsilon \int_D |\nabla v|^2 \, \mathrm{dx} + \frac{\beta}{\varepsilon}\int_D W(u-v) \, \mathrm{dx} \tag{4}$$

where ψ and W are positive functions, decreasing on $\mathbb{R}^-$ and increasing on $\mathbb{R}^+$, vanishing only at 0. Moreover, W is assumed to be continuous and ψ lower semi-continuous. They proved that the functionals AB_ε Γ-converges in $\mathrm{L}^1(D,\mathbb{R}) \times \mathrm{L}^1(D,\mathbb{R})$ to the following relaxation

$$u \mapsto \int_D \psi(u)|\nabla u|^2 \, \mathrm{dx} + \beta \int_{\mathcal{J}_u} \Phi(u^+) + \Phi(u^-) \, \mathrm{d}\mathcal{H}^{\mathrm{N}-1} \tag{5}$$

where $\Phi(t) = 2\left|\int_0^t \sqrt{W(s)} \, \mathrm{ds}\right|$.

The Γ-convergence result with local character we propose is built starting from this result.

Theorem 2.1. *Let D be an open, bounded subset of $\mathbb{R}^N$, and $\alpha > 0$. And let $P_\varepsilon : \mathbb{R} \to \mathbb{R}^+$ be a continuous, non decreasing function such that $\forall x \in (-\infty, 0), P_\varepsilon(x) = 0$ and $\forall x \geq \varepsilon, P_\varepsilon(x) = 1$. We define on $\mathrm{L}^1(D) \times \mathrm{L}^1(D) \to [0, +\infty[$ the functionals*

$$F_\varepsilon(u,v) = \begin{cases} (1+\alpha)^2 \int_D v^{2\alpha}|\nabla u|^2 \, \mathrm{dx} + \varepsilon \int_D |\nabla v|^2 \, \mathrm{dx} & \\ +(1+\alpha)^2 \frac{\beta}{\varepsilon}\int_D (u-v)^{2+4\alpha} \, \mathrm{dx} + \gamma \int_D P_\varepsilon(u) \, \mathrm{dx} & \text{if } u,v \in \mathrm{W}^{1,2}(\Omega) \\ +\infty & \text{else} \end{cases} \tag{6}$$

and

$$F(u,v) = \begin{cases} \int_D |\nabla \tilde{u}|^2 \, \mathrm{dx} + \beta \int_{\mathcal{J}_u} |\tilde{u}^+|^2 + |\tilde{u}^-|^2 \, \mathrm{d}\mathcal{H}^{\mathrm{N}-1} + \gamma\,|\{\tilde{u} > 0\}| & \text{if } u \in \mathrm{SBV}(\Omega) \\ & \text{and } v = u \text{ a.e.} \\ +\infty & \text{else} \end{cases} \tag{7}$$

where $\tilde{u} = u^{1+\alpha}$.

Then F_ε Γ-converges to F in $\mathrm{L}^1(D) \times \mathrm{L}^1(D)$.

Proof: In Acerbi and Braides functional (4) we choose $\psi(t) = t^{2\alpha}$ for $\alpha > 0$. This implies that

$$\int_D u^{2\alpha}|\nabla u|^2 \, \mathrm{dx} = \int_D \frac{\left|\nabla u^{1+\alpha}\right|^2}{(1+\alpha)^2} \, \mathrm{dx}$$

Let us denote $\tilde{u} = u^{1+\alpha}$. Then, identifying (5) with (3) we deduce that $\Phi(t) = t^{2+2\alpha}$. Using the relationship between Φ and W, we finally find that $W(t) = (1+\alpha)^2 t^{2+4\alpha}$.

Thus, to prove $\Gamma - \liminf$ inequality we use both [AB$^+$98, Th. 3.1] and the fact that if $u_\varepsilon \underset{\mathrm{L}^1}{\longrightarrow} u$ then $\liminf \displaystyle\int_D P_\varepsilon(u_\varepsilon)\ \mathrm{dx} \geq |\{u > 0\}|$.

Concerning the $\Gamma - \limsup$ we use the recovery sequences proposed by [AB$^+$98, Prop. 3.7] and remark that $|\{u_\varepsilon > 0\}| = |\{u > 0\}| + \varepsilon \left(T + \dfrac{1}{T}\right)$, which implies that $\displaystyle\int_D P_\varepsilon(u_\varepsilon)\ \mathrm{dx} \underset{\varepsilon\to 0}{\longrightarrow} |\{u > 0\}|$. □

2.2. **Non-local approximation.** We propose in this section an approximation in dimension 1, inspired by the result of Braides and Dal Maso [BDM97] for the Mumford-Shah functional, and adapted to a discretization with finite differences. The functionals we construct are slightly more complicated than those proposed in [BDM97] because functional (3) takes into account the contribution of the traces of u on both sides of the jump set, and not only the difference between them.

We consider the spaces of functions

$$W = \left\{u \in \mathrm{L}^1_{\mathrm{loc}}(\mathbb{R}, \mathbb{R}^+)\ :\ u(x) = 1\ a.e.\ x \in (-\infty, 0), u(x) = 0\ a.e.\ x \in (1, +\infty)\right\}$$

and

$$\mathrm{SBV}^{\frac{1}{2}}(I) = \left\{u \geq 0\ :\ u^2 \in \mathrm{SBV}(I)\right\}.$$

We first prove the following result, which helps for the proof of Theorem 2.3.

Theorem 2.2. *Let $f : [0, +\infty) \to \mathbb{R}^N$ be a continuous, non decreasing function, vanishing only at 0, and satisfying $\lim_{t\to 0^+} \frac{f(t)}{t} = 1$ and $\lim_{t\to\infty} f(t) = 1$. We define on $\mathrm{L}^1_{loc}(\mathbb{R})$ the following functionals :*

$$F_\varepsilon(u) = \begin{cases} \dfrac{\beta}{2\varepsilon}\displaystyle\int_{\mathbb{R}} \left[u^2(x+\varepsilon) + u^2(x-\varepsilon)\right] f\left(\frac{(u(x+\varepsilon) - u(x-\varepsilon))^2}{2\beta\varepsilon(u^2(x+\varepsilon) + u^2(x-\varepsilon)) + \varepsilon^2}\right) \mathrm{dx} & \text{if } u \in W \\ +\infty & \text{else} \end{cases}$$

and

$$F(u) = \begin{cases} \displaystyle\int_{\mathbb{R}} |\nabla u|^2\ \mathrm{dx} + \beta \sum_{x\in\mathcal{J}_u} |u^+|^2 + |u^-|^2 & \text{if } u \in W \cap \mathrm{SBV}^{\frac{1}{2}}(\mathbb{R}) \\ +\infty & \text{else} \end{cases}$$

Then F_ε Γ-converges to F in $\mathrm{L}^1_{loc}(\mathbb{R})$.

The proof follows the steps of Braides' proof in [Bra98, Th. 3.33 and Prop. 3.38], with an additional difficulty, since the energy must take into account the traces of the function on the jump set. The main ideas of the proof are summarized below.

- $\Gamma - \liminf$: we consider $u_\varepsilon \xrightarrow{\mathrm{L}^1_{\mathrm{loc}}} u$ and we replace u_ε by a function v_ε satisfying:
  i) $G_\varepsilon(u_\varepsilon) \geq G_\varepsilon(v_\varepsilon)$,
  ii) $v_\varepsilon \xrightarrow{\mathrm{L}^1_{\mathrm{loc}}} u$,
  iii) $v_\varepsilon \in W \cap \mathrm{SBV}(\mathbb{R})$,
  iv) we can apply lower semi-continuity.
- $\Gamma - \limsup$: we use the density of regular functions (or functions with a finite number of jumps) and constant sequences.

Proof of the $\Gamma - \liminf$ *part*: Let (ε_j) converging to 0 and $(u_j) \subset W$ satisfying $u_j \xrightarrow{a.e.-\mathrm{L}^1_{\mathrm{loc}}} u$. In the spirit of Braides' proof, we construct the sequence of functions

$$g_j(t) = \beta\left[u_j^2(t+\varepsilon) + u_j^2(t-\varepsilon)\right] f\left(\frac{(u_j(t+\varepsilon) - u_j(t-\varepsilon))^2}{2\beta\varepsilon(u_j^2(t+\varepsilon) + u_j^2(t-\varepsilon)) + \varepsilon^2}\right)$$

adapted to energy (3). And let $\Phi_j : [0, 2\varepsilon_j] \to \mathbb{R}$ by defined by

$$\Phi_j(t) = \sum_{k\in\mathbb{Z}} g_j(t + 2k\varepsilon_j),$$

extended by periodicity on $\mathbb{R}$. We notice that only a finite number of terms are non zero in the definition of Φ_j. Moreover,

$$F_{\varepsilon_j}(u_j) = \frac{1}{2\varepsilon_j}\int_{\mathbb{R}} g_j(t)\ \mathrm{dt} = \frac{1}{2\varepsilon_j}\sum_{k\in\mathbb{Z}}\int_{2k\varepsilon_j}^{2(k+1)\varepsilon_j} g_j(t)\ \mathrm{dt} = \frac{1}{2\varepsilon_j}\sum_{k\in\mathbb{Z}}\int_0^{2\varepsilon_j} \Phi_j(t)\ \mathrm{dt} = \int_0^1 \Phi_j(t)\ \mathrm{dt}.$$

Substracting a subsequence if necessary we can assume that

$$\lim_{j\to+\infty} F_{\varepsilon_j}(u_j) = M < +\infty.$$

Let us fix $\eta > 0$ and introduce the sets

$$A_j = \left\{y \in (0,1)\ :\ \Phi_j(y) \le F_{\varepsilon_j}(u_j) + \eta\right\} \text{ and } B_j = (0,1)\backslash A_j.$$

Then

$$|B_j| \le \frac{1}{F_{\varepsilon_j}(u_j)+\eta}\int_{B_j} \Phi_j(y)\ \mathrm{dy} \le \frac{1}{F_{\varepsilon_j}(u_j)+\eta}\int_0^1 \Phi_j(y)\ \mathrm{dy} = \frac{F_{\varepsilon_j}}{F_{\varepsilon_j}(u_j)+\eta} \xrightarrow[j\to+\infty]{} \frac{M}{M+\eta} < 1.$$

We can asume that for j large enough their exists a constant C, independant of j, such that

$$|B_j| \le C < 1,$$

implying that

$$|A_j| \ge 1 - C > 0.$$

We introduce the piecewice constant functions

$$T_y^{\varepsilon} v(x) = v\left(y + \left[\frac{x-y}{\varepsilon}\right]\right),$$

constant on every interval of the form $(y + k\varepsilon, y + (k+1)\varepsilon)$, $k \in \mathbb{Z}$. Then, in view of [Bra98, Lem. 3.36], for almost every y we have

$$T_y^{\varepsilon_j} u_j \xrightarrow{\mathrm{L}^1_{\mathrm{loc}}} u.$$

If we denote $P_j(y) = \|T_y^{\varepsilon_j} u_j - u\|_{\mathrm{L}^1}$ then we have

$$P_j \xrightarrow{a.e.-\mathbb{R}} 0.$$

Using Egorov's theorem,

$$\exists E \text{ t.q. } |E| \le \frac{1-C}{2} \text{ and } P_j \xrightarrow[\text{unif.}]{\mathbb{R}\backslash E} 0.$$

So their exists $y_j \in A_j\backslash E$ such that

$$T_{y_j}^{\varepsilon_j} u_j \xrightarrow{\mathrm{L}^1_{\mathrm{loc}}(\mathbb{R})} u,$$

implying

$$F_{\varepsilon_j}(u_j) + \eta \ge \Phi_j(y_j). \tag{8}$$

To simplify notations, we assume that $y_j = 0$ (up to a small translation, and a rescaling to remain in W). We introduce, as in [BDM97]

$$J_j^1 = \left\{k\ :\ \frac{(u_j(2(k+1)\varepsilon_j) - u_j(2k\varepsilon_j))^2}{2\beta\varepsilon_j(u_j^2(2k\varepsilon_j) + u_j^2(2(k+1)\varepsilon_j)) + \varepsilon_j^2} \le 1\right\}$$

and

$$J_j^2 = {J_j^1}^C.$$

We define new functions $v_j \in \mathrm{SBV}(\mathbb{R})$ which have the same limit u in L^1 and energy lower than u_j, such that

$$v_j(t) = \begin{cases} \text{an affine interpolation of } u_j \text{ on } (2k\varepsilon_j, 2(k+1)\varepsilon_j) & \text{if } k \in J_j^1 \\ \text{piecewise constant} & \text{if } k \in J_j^2 \end{cases}$$

Following [Bra98, Rem. 3.37], we find that

$$v_j \xrightarrow{\mathrm{L}^1_{\mathrm{loc}},\ \mathrm{L}^1(0,1)} u.$$

On the other hand we have

$$\begin{aligned} F_{\varepsilon_j} + \eta &\ge \sum_{k\in J_j^1} \frac{1}{4\varepsilon_j^2}\left(u_j(2(k+1)\varepsilon_j) - u_j(2k\varepsilon_j)\right)^2 + \sum_{k\in J_j^2} \beta\left[u_j(2(k+1)\varepsilon_j) + u_j(2k\varepsilon_j)\right] \\ &= \int_{\mathbb{R}} |\nabla v_j|^2\ \mathrm{dx} + \beta \sum_{t\in\mathcal{J}_{v_j}} |v_j^+(t)|^2 + |v_j^-(t)|^2. \end{aligned}$$

Passing to the limit on j and using the lower semi-continuity theorem in $\mathrm{SBV}^{\frac{1}{2}}$ we deduce that $u \in \mathrm{SBV}^{\frac{1}{2}}$ and

$$\liminf_j G_{\varepsilon_j} \ge \int_{\mathbb{R}} |\nabla u|^2\ \mathrm{dx} + \beta \sum_{t\in\mathcal{J}_u} |u^+|^2 + |u^-|^2 = G(u) - \eta.$$

Proof of the $\Gamma-\limsup$ *part*: By density, it is enough to consider $u \in \mathrm{SBV}(\mathbb{R}) \cap W$, such that u has only one jump at $t_0 \in (0,1)$ (or a finite number of jumps), $u \in \mathrm{C}^1(\mathbb{R}\backslash \mathcal{J}_u)$, and $u(x) \leq M$, $u(x) \geq \alpha > 0$ *a.e.* in $\{x \ : \ u(x) > 0\}$.

We evaluate

$$\begin{aligned}
F_\varepsilon(u) &\approx \frac{\beta}{2\varepsilon}\int_{-\varepsilon}^{t_0-\varepsilon} \left[u^2(x+\varepsilon)+u^2(x-\varepsilon)\right] \frac{(u(x+\varepsilon)-u(x-\varepsilon))^2}{2\beta\varepsilon(u^2(x+\varepsilon)+u^2(x-\varepsilon))+\varepsilon^2} \ \mathrm{dx} \\
&+ \frac{\beta}{2\varepsilon}\int_{t_0-\varepsilon}^{t_0+\varepsilon} \left[u^2(x+\varepsilon)+u^2(x-\varepsilon)\right] \ \mathrm{dx} \\
&+ \frac{\beta}{2\varepsilon}\int_{t_0+\varepsilon}^{1+\varepsilon} \left[u^2(x+\varepsilon)+u^2(x-\varepsilon)\right] \frac{(u(x+\varepsilon)-u(x-\varepsilon))^2}{2\beta\varepsilon(u^2(x+\varepsilon)+u^2(x-\varepsilon))+\varepsilon^2} \ \mathrm{dx} \\
&\xrightarrow[\varepsilon\to 0]{} \int_0^1 |\nabla u|^2 \ \mathrm{dx} + \beta\left[|u^+(t_0)|^2+|u^-(t_0)|^2\right].
\end{aligned}$$

□

Theorem 2.3. *Let* $f : [0,+\infty) \to \mathbb{R}^N$ *be a continuous, non decreasing function, vanishing only at 0, and satisfying* $\lim\limits_{t\to 0^+} \frac{f(t)}{t} = 1$ *and* $\lim\limits_{t\to\infty} f(t) = 1$. *And let* $P_\varepsilon : \mathbb{R} \to \mathbb{R}^+$ *be a continuous, non decreasing function such that* $\forall x \in (-\infty, 0), P_\varepsilon(x) = 0$ *and* $\forall x \geq \varepsilon, P_\varepsilon(x) = 1$. *We define on* $\mathrm{L}^1_{loc}(\mathbb{R})$ *the following functionals :*

$$G_\varepsilon(u) = \begin{cases} \dfrac{\beta}{2\varepsilon}\displaystyle\int_{\mathbb{R}} \left[u^2(x+\varepsilon)+u^2(x-\varepsilon)\right] f\left(\frac{(u(x+\varepsilon)-u(x-\varepsilon))^2}{2\beta\varepsilon(u^2(x+\varepsilon)+u^2(x-\varepsilon))+\varepsilon^2}\right) \ \mathrm{dx} \\ \qquad\qquad + \gamma\displaystyle\int_{\mathbb{R}} P_\varepsilon(u) \ \mathrm{dx} & \text{if } u \in W \\ +\infty & \text{else} \end{cases} \tag{9}$$

and

$$G(u) = \begin{cases} \displaystyle\int_D |\nabla u|^2 \ \mathrm{dx} + \beta\int_{\mathcal{J}_u} |u^+|^2+|u^-|^2 \ \mathrm{d}\mathcal{H}^{\mathrm{N}-1} + \gamma\,|\{u>0\}| & \text{if } u \in W\cap \mathrm{SBV}^{\frac12}(\mathbb{R}) \\ +\infty & \text{else} \end{cases} \tag{10}$$

Then G_ε Γ*-converges to* G *in* $\mathrm{L}^1_{loc}(\mathbb{R})$.

Proof:

The proof is immediate since the recovery sequence is constant for $u \in \mathrm{SBV}^{\frac12}$ and $\displaystyle\int_I \psi_\varepsilon(u_\varepsilon) \ \mathrm{dx} \xrightarrow[\varepsilon\to 0]{}$ $|\{u>0\}|$, while in general, if $u_\varepsilon \xrightarrow{\mathrm{L}^1} u$ then $\liminf \displaystyle\int_I \psi_\varepsilon(u_\varepsilon) \ \mathrm{dx} \geq |\{u>0\}|$. □

3. Numerical results in 1D

In this section, we consider a particular case in dimension 1 for which we can compute analytically the solution. Then we present some numerical results of the minimization of the approximations of (3) presented in section 2.

3.1. **Analytic computation in dimension 1.** Let $D = [0,1]$, $K = \{0\}$ and $g \equiv 1$ on K. In this particular case, Ω is an interval $[0, L]$, $0 < L < 1$, and solves

$$\min_L \min_{u(0)=1} \int_0^L |u'|^2 \ \mathrm{dx} + \beta u^2(L) + \gamma\,|\{u>0\}|. \tag{11}$$

A solution u of (11) is harmonic. Using the constraint on 0 and Robin boundary condition in L, we find out that energy at L is equal to

$$E(L) = a^2L + \beta(aL+1)^2 + \gamma L = \frac{\beta}{(1+\beta L)} + \gamma L.$$

Solving Euler-Lagrange equation, we find that

$$L = \frac{1}{\beta}\left(\frac{\beta}{\sqrt{\gamma}} - 1\right).$$

A solution of (11) for $\beta = 2$ and $\gamma = 1$ is finally

$$u(x) = \begin{cases} -x+1 & \text{if } x \in \left[0, \dfrac{1}{2}\right] \\ 0 & \text{else} \end{cases} \tag{12}$$

In this case, optimal energy is equal to

$$\int_0^{1/2} |u'|^2 \, \mathrm{dx} + \beta u\left(\frac{1}{2}\right) + |\{u > 0\}| = \frac{3}{2}. \tag{13}$$

3.2. **Numerical aspects.** We discretize $[0,1]$ using $n+1$ points $x_i = i.h$ $\forall i \in \{0, ..., n\}$ where $h = \frac{1}{n}$. And we denote $u(x_i) = u_i$ $\forall i \in \{0, ..., n\}$. We approximate the first and second derivatives of u using finite differences

$$u_i' = \frac{u_{i+1} - u_{i-1}}{2h},$$
$$u_i'' = \frac{u_{i+1} - 2u_i + u_{i-1}}{h^2}.$$

Functionals (6) and (9) are non-convex, therefore we use a gradient descent method, alternately solving for u and v for the local approximation (6). Moreover, we choose $P_\varepsilon(x) = \max\left(0, \min\left(\frac{x}{\varepsilon}, \varepsilon\right)\right)$ and $f(x) = \max(0, \min(x, \varepsilon))$. And to reproduce Γ-convergence process numerically, we choose an initial value ε_1 large enough to detect the jump and then refine it with a ratio ε_r until a final value ε_2. We denote by $\varepsilon = \varepsilon_1 \searrow \varepsilon_2$ this process.

Var u: vector, (v, v'): vectors, ε: real ;
begin
  $u \leftarrow \max\left(0, \min\left(1, \dfrac{1-2\varepsilon-x}{1-4\varepsilon}\right)\right)$, $v \leftarrow u$;
  $\varepsilon \leftarrow \varepsilon_1$;
  while $\varepsilon \geq \varepsilon_2$ **do**
    repeat
      $u^{n+1} \leftarrow u^n - \delta_u \frac{\mathrm{dL}_\varepsilon}{\mathrm{du}}$;
      `// Only for the local approximation (6).`
      $v' \leftarrow v$;
      $v^{n+1} \leftarrow v^n - \delta_v \frac{\mathrm{dL}_\varepsilon}{\mathrm{dv}}$;
      constraint(u);
    until $\|v - v'\|$ *is small*;
    $\varepsilon \leftarrow \varepsilon / \varepsilon_r$;
  end
  return (u, v) ;
end

Algorithm 1: OPTIMIZE-R($(\alpha, \beta, \gamma, \varepsilon_1, \varepsilon_2, \varepsilon_r)$: reals)

3.3. **Acerbi-Braides type approximation.** Local approximation (6) depends on two functions u and v. In this functional, v should approximate u excepted on its jump set, where v has to be equal to 0. We observe in figure 1 that v jumps just before u does, as expected. Moreover, jump of u is quite well localised at point $\frac{1}{2}$. However, v does not match u exactly on regular parts.

Actually, if we look at the recovery sequences proposed by Acerbi and Braides for the proof of [AB+98, Th. 3.1], we observe that the interface should appear on an interval of length $\frac{\varepsilon}{T}$. A direct computation shows that if we want the interface to appear on 5 points when $\alpha \approx 0$, *i.e.* $5h \leq \frac{\varepsilon}{T}$, then $\varepsilon \geq 0.1$ for 2000 points in $[0,1]$ and $T = 40$. Thus if we want to decrease ε, we need to refine the gridstep faster than ε tends to 0, which leads to numerical difficulties.

3.4. **Non local approximation.** Figure 2 shows the results of the minimization of functional (9) with different initializations. The final energies are listed in table 1.

We observe that the non local approximation leads to affine solutions with an expected behavior. Nevertheless, the optimization algorithm is very sensitive to local minima (see Table 1). We observe that an oscillating initialization leads to better solutions. A way to outperform these results is to rerun the algorithm using a perturbation of the numerical optimizer u^* as initialization and iterate this process until convergence to a fixed solution. Figure 3 shows the result of minimization using this process.

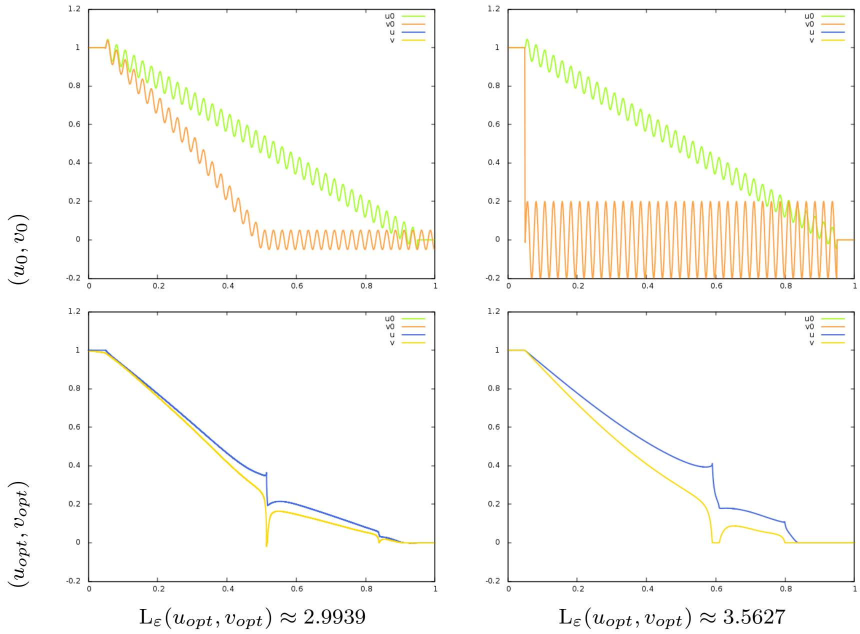

FIGURE 1. Minimization of (6) with various initializations, 10000 points and $\varepsilon = 1.0 \searrow 0.006$.

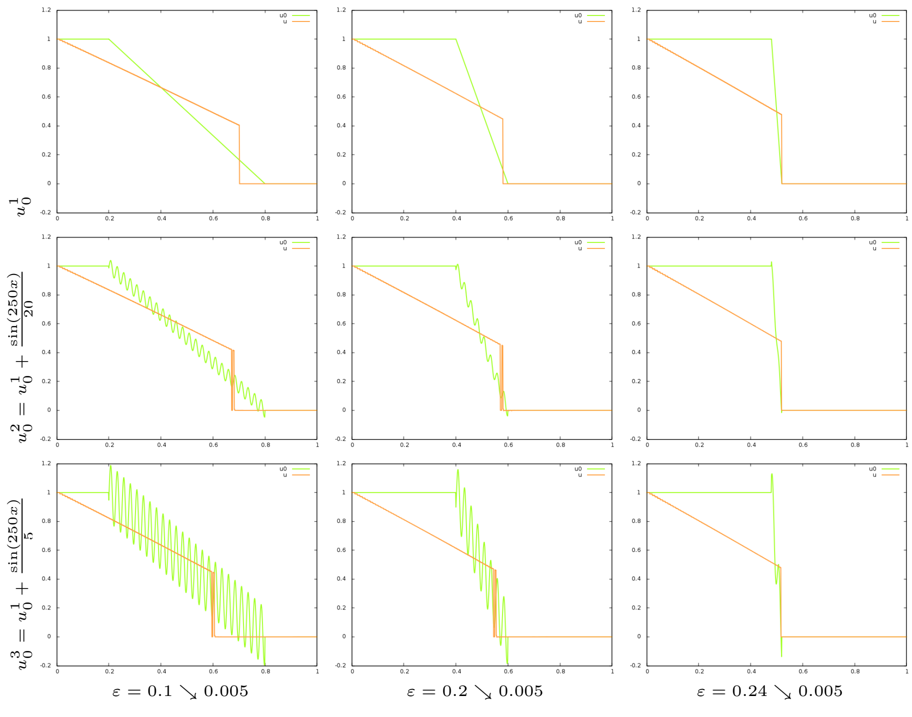

FIGURE 2. Minimization of (9) with various initializations and values of ε_1, with 1000 points.

TABLE 1. Final values of energy for the experiments shown in figure 2. Expected value (13): $\frac{3}{2}$.

	$\varepsilon = 0.1 \searrow 0.005$	$\varepsilon = 0.2 \searrow 0.005$	$\varepsilon = 0.24 \searrow 0.005$
(9) with u_0^1	1.489	1.520	1.473
(9) with u_0^2	1.489	1.5054	1.473
(9) with u_0^3	1.471	1.503	1.473

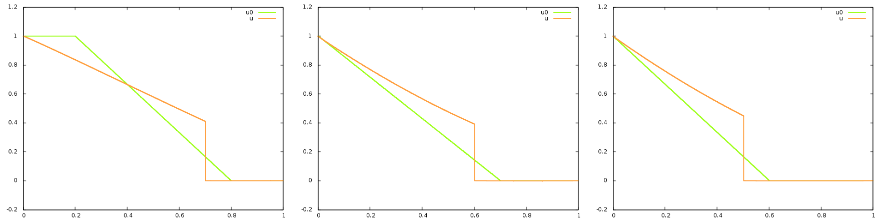

FIGURE 3. Minimization of (9) using a fixed point algorithm. From left to right: first processing; second processing using a perturbation of the first optimum as initialization; third processing using a perturbation of the second optimum as initialization.

4. The Two Dimensional Case

In dimension two, it is possible to solve directly the problem (2) using a method based on fundamental solutions, if we restrict ourselves to simply connected shapes Ω and particular shapes of K. Indeed, we are looking for a harmonic function which satisfies the given boundary conditions of type Dirichlet on the inner boundary and Robin on the exterior boundary. Following an approach similar to the one used in [Bog16] we may search for linear combinations of a family of radial harmonic functions which approximately satisfy the boundary conditions. The advantage is that such a linear combination of harmonic functions will satisfy the partial differential equation (2) analytically inside the domain. Error bounds on the approximation can be given in terms of the error corresponding to the boundary conditions. We describe below the numerical framework for solving (2), a basic error bound result and some examples of the optimization of the outer boundary $\partial\Omega$ given the inner set K and a source function g defined on ∂K.

In dimension two, given a source point $y_0 \in \mathbb{R}^2$, the function $\phi(x) = \log \|x - y_0\|$ is harmonic in $\mathbb{R}^2 \setminus \{y_0\}$ and radial about y_0. If we choose a family of source points $y_1, ..., y_M$ and we denote $\phi_i(x) = \log \|x - y_i\|$ then any linear combination

$$\alpha_1 \phi_1 + ... + \alpha_M \phi_M$$

is harmonic in $\mathbb{R}^2 \setminus \{y_1, ..., y_M\}$. Thus, if in our case the source points y_i are all chosen outside $\Omega \setminus K$ then choosing u as a linear combination of ϕ_i will be harmonic in $\Omega \setminus K$. In our problem (2) we also have boundary conditions and in order to impose those we consider a discretization of the boundary. Unlike the result presented in [Bog16] we are dealing here with domains which are not simply connected. Below we use ideas from [AA09] and [AV10] to efficiently choose the source points and the discretization of the boundary $\partial\Omega$ and ∂K on which we impose the corresponding boundary conditions.

We consider two positive integers M_1 and M_0 and we consider points $x_1, ..., x_{M_1}$ chosen on $\partial\Omega$ and points $x_{M_1+1}, ..., x_{M_1+M_0}$ chosen on ∂K. In our computations we will only deal with cases where $\partial\Omega$ and ∂K are parametrized using radial functions $\rho_\Omega, \rho_K : [0, 2\pi) \to \mathbb{R}_+$. In this case we choose the points x_i corresponding to an equal angle division of the boundaries $\partial\Omega$ and ∂K. Following ideas from [AV10] we choose the source points on normals to $\partial\Omega$ and ∂K at points x_i, at a fixed distance $r = 0.1$ from these respective boundaries. Therefore we have $y_i = x_i + 0,1 \cdot \vec{n}(x_i)$ (examples of distribution of points can be seen in Figure 4). Since given coefficients $\alpha_i, i = 1, ..., M_1 + M_0$ the function $u = \sum_{i=1}^{M_0+M_1} \alpha_i \phi_i$ is defined

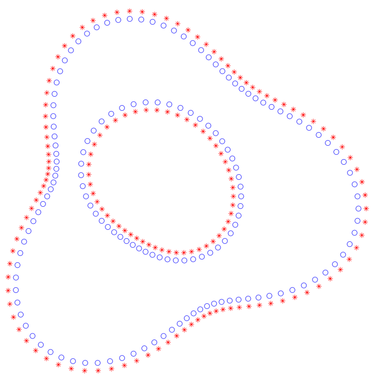

FIGURE 4. Example of a distribution of source and evaluation points on the exterior and inner boundaries

analytically, we can compute its gradient

$$\nabla u(x) = \sum_{i=1}^{M_0+M_1} \alpha_i \frac{x-y_i}{\|x-y_i\|}.$$

Therefore the Robin boundary condition on $\partial\Omega$ and the Dirichlet boundary condition on ∂K evaluated at points $x_i, i = 1, ..., M_0 + M_1$ can all be expressed as a system of linear equations in terms of the coefficients $\alpha_i,\ i = 1, ..., M_0 + M_1$. The Robin conditions on $\partial\Omega$ evaluated at $x_i,\ i = 1, ..., M_1$ are given by

$$\sum_{j=1}^{M_1+M_0} \alpha_j \left(\frac{x_i - y_j}{\|x_i - y_j\|} \cdot \vec{n}(x_i) + \beta \log \|x_i - y_j\| \right) = 0,$$

for $i = 1, ..., M_1$. The Dirichlet boundary conditions on ∂K evaluated at $x_i,\ i = M_1 + 1, ..., M_1 + M_0$ can be imposed using

$$\sum_{j=1}^{M_0+M_1} \alpha_j \log \|x_i - y_j\| = g(x_i).$$

Thus we can define the matrices $A = (\frac{x_i-y_j}{\|x_i-y_j\|} \cdot \vec{n}(x_i) + \beta \log \|x_i - y_j\|), 1 \leq i \leq M_1,\ 1 \leq j \leq M_0 + M_1$ and $B = \log \|x_i - y_j\|, M_1 + 1 \leq i \leq M_0 + M_1,\ 1 \leq j \leq M_0 + M_1$. Then the Robin and Dirichlet boundary conditions can be imposed via the system

$$\begin{pmatrix} A \\ B \end{pmatrix} \vec{x} = \begin{pmatrix} \vec{0} \\ \vec{g} \end{pmatrix} \tag{14}$$

where $\vec{x} = (\alpha_j)_{j=1}^{M_0+M_1}$ contains the coefficients of the linear combination of the fundamental solutions and $\vec{g} = (g(x_i))_{M_1+1 \leq i \leq M_0+M_1}$. Therefore, solving (14) will give us the coefficients α_j for the function

$$u = \sum_{j=1}^{M_0+M_1} \alpha_j \phi_j,$$

function which is harmonic in $\Omega \setminus K$ and satisfies the boundary conditions at points $x_i,\ 1 \leq i \leq M_0 + M_1$.

It is possible to find error bounds regarding our numerical method by using classical methods, like the ones used in [GC99]. Suppose that u_ε satisfies the approximate partial differential equation

$$\begin{cases} -\Delta u_\varepsilon = 0 & \text{in } \Omega \setminus K \\ \partial_n u_\varepsilon + \beta u_\varepsilon = f_\varepsilon & \text{on } \partial\Omega \\ u_\varepsilon = g_\varepsilon & \text{on } \partial K. \end{cases} \tag{15}$$

The variational form of the above equation is given by

$$\int_{\Omega\setminus K} \nabla u_\varepsilon \nabla \phi + \beta \int_{\partial\Omega} u_\varepsilon \phi + \int_{\partial K} u_\varepsilon \phi = \int_{\partial\Omega} f_\varepsilon \phi + \int_{\partial K} g_\varepsilon \phi \quad \text{for every} \quad \phi \in H^1(\Omega). \tag{16}$$

Theorem 4.1. *Let $g_\varepsilon \in L^2(\partial K)$ and $f_\varepsilon \in L^2(\partial\Omega)$ and that $g_\varepsilon, f_\varepsilon, \Omega, K$ are regular enough such that $u_\varepsilon \in C_2(\Omega \setminus K) \cap C(\overline{\Omega \setminus K})$. Then if u_ε solves the equation* (15) *then there exists a constant $C(\Omega, K)$ such that*

$$\|u_\varepsilon\|_{L^2(\Omega\setminus K)} \leq C(\Omega, K)(\|f_\varepsilon\|_{L^2(\partial\Omega)} + \|g_\varepsilon\|_{L^2(\partial K)})$$

Moreover, the constant $C(\Omega, K)$ can be computed explicitly in terms of the sets Ω, K.

Therefore, if we have an upper bound on the terms f_ε and g_ε, we can deduce estimates on the solution u_ε. In particular, if u_ε is the difference between the exact solution of (2) and the numerical approximation given by the method of fundamental solutions, it is possible to deduce numerical error bounds by providing estimates of the errors $f_\varepsilon, g_\varepsilon$ made in the approximation of the boundary conditions. We note that the regularity assumptions needed for Theorem 4.1 to be valid are true in our numerical simulations.

Proof: Taking $\phi = u_\varepsilon$ in (16) and applying the Cauchy-Schwarz inequality we get

$$\|\nabla u_\varepsilon\|^2_{L^2(\omega\setminus K)} + \beta \|u_\varepsilon\|^2_{L^2(\partial\Omega)} + \|u_\varepsilon\|^2_{L^2(K)} \leq \|f_\varepsilon\|_{L^2(\partial\Omega)} \|u_\varepsilon\|_{L^2(\partial\Omega)} + \|g_\varepsilon\|_{L^2(\partial K)} \|u_\varepsilon\|_{L^2(\partial K)}.$$

We denote, for simplicity $C_\varepsilon = \|u_\varepsilon\|_{L^2(\partial\Omega\cup\partial K)}$. Using the inequality $(a+b)^2 \leq 2(a^2+b^2)$ we get that

$$\min\{\beta, 1\} C_\varepsilon^2 \leq 2 \min\{\beta, 1\}(\|u_\varepsilon\|^2_{L^2(\partial\Omega)} + \|u_\varepsilon\|^2_{L^2(K)}) \leq 2(\|f_\varepsilon\|_{L^2(\partial\Omega)} + \|g_\varepsilon\|_{L^2(\partial K)}) C_\varepsilon$$

This allows us to find an explicit upper bound for C_ε in terms of the L^2 norms $\|f_\varepsilon\|_{L^2(\partial\Omega)}$ and $\|g_\varepsilon\|_{L^2(\partial K)}$.

Next, it is possible, to get estimates of $\|u_\varepsilon\|_{L^2(\Omega\setminus K)}$ in terms of C_ε. We follow classical works like [GC99], which give methods to find *a priori* error estimates for Poisson's equation. The key ingredient is the following inequality which can be found, for example in [Gus99, p. 74]. If $-\Delta u_\varepsilon = 0$ then there exists a constant $c(\Omega \setminus K)$, related to the first Steklov eigenvalue of the biharmonic operator on $\Omega \setminus K$, such that

$$\int_{\Omega\setminus K} u_\varepsilon^2 \leq c(\Omega \setminus K) \int_{\partial\Omega\cup\partial K} u^2.$$

For a proof of a more general version of this estimate, with a non-zero right-hand side in the Poisson equation, see [Gus99, p. 74]. Finally, we conclude that

$$\|u_\varepsilon\|_{L^2(\Omega\setminus K)} \leq \frac{c(\Omega\setminus K)^{1/2}}{\min\{\beta, 1\}}(\|f_\varepsilon\|_{L^2(\partial\Omega)} + \|g_\varepsilon\|_{L^2(\partial K)})$$

which finishes the proof. □

In order to perform the optimization of (1) we need to compute the shape derivative of

$$E(\Omega, u) = \int_\Omega |\nabla u|^2 + \beta \int_{\partial\Omega} u^2 d\sigma,$$

where u solves (2). Following an approach similar to the one in [CDK13, Prop 5.1] we prove the following shape derivative formula. For simplicity we place ourselves in the case where both Ω and the vector field V inducing a perturbation of $\partial\Omega$ are smooth enough. These assumptions will be satisfied in our numerical simulations.

Theorem 4.2. *Suppose Ω is smooth and let V be a smooth vector field giving a perturbation of $\partial\Omega$ then the derivative of the energy $E(\Omega, u)$ defined above in the direction of V is given by*

$$\frac{dE(\Omega)}{dV} = \int_{\partial\Omega} |\nabla_\tau u|^2 V.n - \beta^2 \int_{\partial\Omega} u^2 V.n + \beta \int_{\partial\Omega} \mathcal{H} u^2 V.n, \tag{17}$$

where ∇_τ represents the tangential gradient with respect to $\partial\Omega$ and $\mathcal{H}$ is the mean curvature of Ω.

Proof: Using the fact that u satisfies (2) and performing an integration by parts we find that

$$E(\Omega, u) = -\int_\Omega u\delta u + \int_{\partial\Omega} \partial_n u \; ud\sigma + \int_{\partial K} \partial_n u \; ud\sigma + \beta \int_{\partial\Omega} u^2 d\sigma = \int_{\partial K} \partial_n u \; ud\sigma.$$

This latter expression has the advantage of computing the energy as an integral on a fixed domain. Therefore the derivative of $E(\Omega, u)$ is given by

$$\frac{dE(\Omega)}{dV} = \int_{\partial K} \partial_n u' \cdot ud\sigma + \int_{\partial K} \partial_n u \cdot u' d\sigma,$$

where u' satisfies the adjoint equation [CDK13]

$$\begin{cases} -\Delta u' &= 0 & \text{in } \Omega\setminus K \\ u' &= 0 & \text{on } \partial K \\ \partial_n u' + \beta u' &= (-\beta\partial_n u - \beta\mathcal{H}u + \Delta_\tau u)V.n + \nabla_\tau u \cdot \nabla_\tau (V.n) & \text{on } \partial\Omega \end{cases}, \tag{18}$$

where ∇_τ and Δ_τ represent the tangential gradient and the Laplace-Beltrami operators associated to $\partial\Omega$. Therefore it remains to compute

$$\frac{dE(\Omega)}{dV} = \int_{\partial K} \partial_n u' \cdot ud\sigma,$$

since $u' = 0$ on ∂K. Taking u as test in the equation of u' and conversely we get

$$\int_{\Omega\setminus K} \nabla u' \cdot \nabla u - \int_{\partial K} \partial_n u' \cdot ud\sigma - \int_{\partial\Omega} \partial_n u' \cdot ud\sigma = 0$$

and

$$\int_{\Omega\setminus K} \nabla u \cdot \nabla u' - \int_{\partial K} \partial_n u \cdot u' d\sigma - \int_{\partial\Omega} \partial_n u \cdot u' d\sigma = 0.$$

Subtracting these two relations we get

$$\int_{\partial K} \partial_n u' \cdot ud\sigma = \int_{\partial\Omega} \partial_n u \cdot u' d\sigma - \int_{\partial\Omega} \partial_n u' \cdot ud\sigma.$$

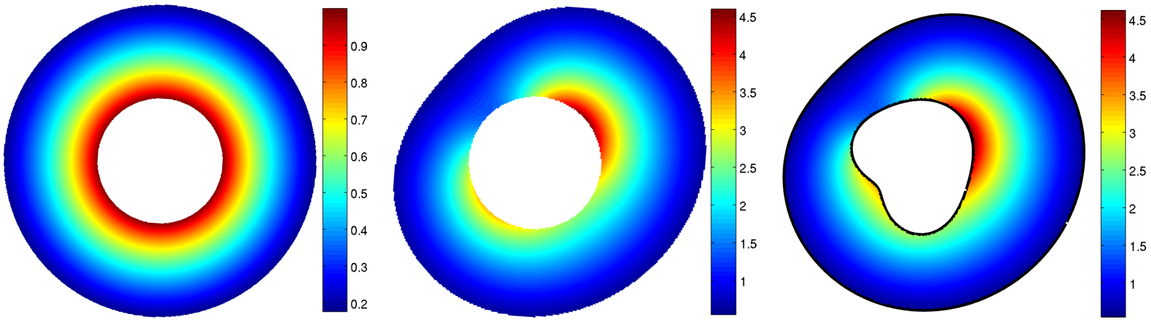

FIGURE 5. Numerical results obtained using fundamental solutions: radial case, $g \equiv 1$, K disk and g non-constant, general K and general g

Now we use the boundary conditions of u and u' on $\partial\Omega$ to conclude.

$$\begin{aligned}\int_{\partial B} \partial_n u' \cdot u d\sigma = &-\int_{\partial\Omega} \beta u \cdot u' d\sigma + \beta_{\partial\Omega} u' \cdot u d\sigma + \beta \int_{\partial\Omega} u' \cdot u d\sigma \\ &+ \beta \int_{\partial\Omega} \partial_n u \cdot u V.n d\sigma + \beta \int_{\partial\Omega} \mathcal{H} u \cdot u V.n d\sigma \\ &- \int_{\partial\Omega} \Delta_\tau u \cdot u V.n d\sigma - \int_{\partial\Omega} \nabla_\tau u \cdot \nabla_\tau (V.n) \cdot u \\ &= \int_{\partial\Omega} |\nabla_\tau u|^2 V.n d\sigma - \beta^2 \int_{\partial\Omega} u^2 V.n d\sigma + \beta \int_{\partial\Omega} \mathcal{H} u^2 V.n,\end{aligned}$$

where we have used the fact that by integrating by parts on $\partial\Omega$ we have

$$-\int_{\partial\Omega} \Delta_\tau u \cdot u V.n d\sigma = \int_{\partial\Omega} \nabla_\tau u \cdot \nabla_\tau u V.n d\sigma + \int_{\partial\Omega} \nabla_\tau u \cdot \nabla_\tau (V.n) u d\sigma.$$

This concludes the proof of (17). □

Note that the shape-derivative formula (17) is similar to the shape derivative of the Wentzell eigenvalue [DKL16], which also contains tangential and normal components of the gradient of the solution u. As already seen in [Bog16], a big advantage of using the fundamental solution formulation is that it allows us to compute the integrands in (17) explicitly. Using a simple order one quadrature formula in order to compute the integrals gives enough precision for the numerical algorithms to converge. The use of other numerical methods may induce higher errors in the computation of the derivative.

In our numerical computation we use the hypothesis that the shape Ω to be optimized is star-shaped and can be parametrized using a radial function $\rho_\Omega : [0, 2\pi) \to [0, +\infty)$. As in other works like [Ost10], [AF12] or [Bog16], we consider the expansion of ρ_Ω into Fourier series which we then truncate to a finite number of coefficients

$$\rho_\Omega(\theta) \approx a_0 + \sum_{i=1}^N a_k \cos(k\theta) + \sum_{i=1}^N b_k \sin(k\theta).$$

In this way we have described Ω using $2N+1$ parameters. Using the shape derivative formula (17) and the fact that perturbing a Fourier coefficient induces a particular deformation field of the boundary we can find the derivative of the energy $E(\Omega, u)$ in terms of each of the Fourier coefficients:

$$\begin{aligned}\frac{\partial E}{\partial a_k} &= \int_0^{2\pi} \left(|\nabla_\tau u|^2 - \beta^2 u^2 + \beta \mathcal{H} u^2\right) \cos(k\theta) d\theta \\ \frac{\partial E}{\partial b_k} &= \int_0^{2\pi} \left(|\nabla_\tau u|^2 - \beta^2 u^2 + \beta \mathcal{H} u^2\right) \sin(k\theta) d\theta.\end{aligned}$$

We are now ready to run a quasi-Newton algorithm in order to optimize $E(\Omega, u)$ in terms of the first $2N+1$ Fourier coefficients. We perform the optimization in Matlab using the library [Sch12] with an algorithm of the type LBFGS.

1. The Radial Case. We start with the case where K is the unit disk and $g \equiv 1$ on ∂K. In this case, the solution Ω is a disk of radius $t > 1$. Therefore in this case u is radial and $u(1) = 1$. Thus we may search for functions of the form $u(r) = a \ln r + 1$. We recall below a direct computation taken from [Mar17, Section 6.6.1, p 145] which can give the explicit solution of (1) given β and γ. We find that

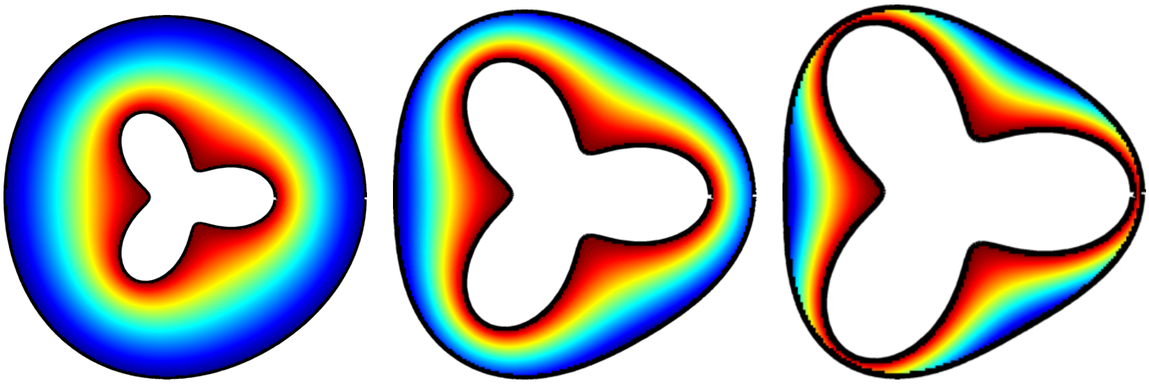

FIGURE 6. Numerical tests for K non-convex and $\gamma = 0.1, 0.5, 1$

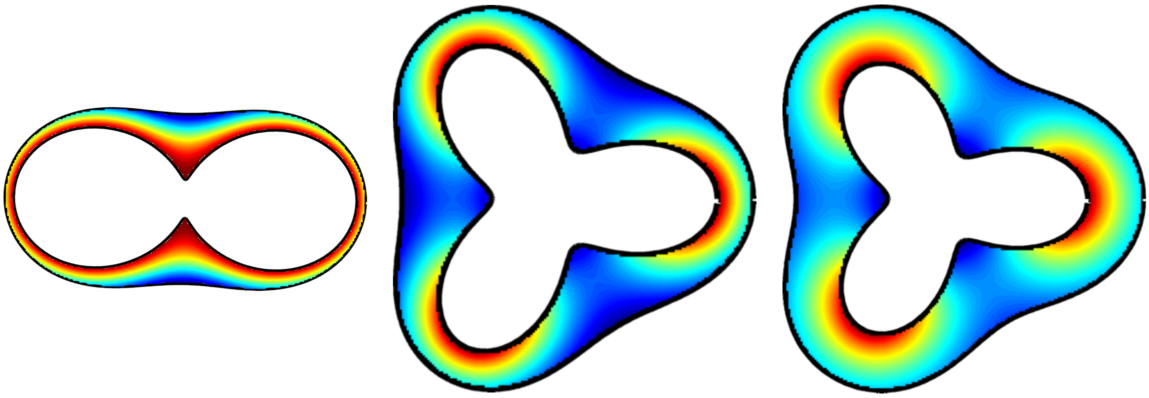

FIGURE 7. Numerical tests for K non-convex, with variable source terms. Note that the optimal shape Ω can become non-convex.

the explicit value of the energy in terms of t is

$$E(t) = \frac{2\pi}{1/(t\beta) + \ln t} + \gamma \pi t^2.$$

For example, if $\beta = 2$ and $\gamma = 0.1$ then the minimum of the energy is attained in $t \approx 2.52$ and the energy in this case is equal to $E(t) = 7.59$. We run our shape optimization algorithm for $\beta = 2$ and $\gamma = 0.1$ and we obtain a disk, as expected, and the optimal energy agrees to 10^{-4} to the value obtained when optimizing $E(t)$ above. The result can be visualized in Figure 5.

2. General source term. We start by generalizing the source term g on ∂K. As the minimization of the energy (1) is related to an insulation problem, we expect that the optimal shape Ω would be thicker on parts of ∂K which have a higher value of the source term. In our computations below we used $g(\theta) = 3 + \sin(2\theta) + 0.7\cos(\theta) - 0.2\cos(3\theta)$ where θ is the parameter in the radial parametrization of ∂K. We perform the optimization for parameters $\beta = 2$ and $\gamma = 1.1$. The result is presented in Figure 5.

3. General K and source term. It is possible to fully generalize the choices of K and the source term g on ∂K. An initial example can be seen in Figure 5. We may wonder if it is possible to obtain non-convex optimal shapes Ω. As suggested in [CK16] when K is convex and $g \equiv 1$ it is likely that the optimal shape Ω is convex. One may wonder what happens if K is non-convex. In Figure 6 we investigate what happens if K is a particular non-convex shape and we increase the parameter γ, allowing less and less area. We notice that the optimal shape remains convex in this case. One aspect which may prevent Ω from becoming non-convex when $g \equiv 1$ is the fact that non-convex parts of ∂K generate more heat and therefore need to be better insulated. It is possible to observe non-convex optimal shapes even if $g \equiv 1$ if we have an elongated non-convex source K, as can be seen in Figure 7. If, in addition, we consider non-convex source domains K with small heat sources on the reentrant part, we may obtain non-convex optimal shapes Ω, as can be seen in Figure 7.

Remarks concerning the numerical results in 2D. The simulations performed above allow us to find couples (Ω, u) which solve (1). In the simulations we can see the shape of the optimizers as well as the function u which solves the partial differential equation with Robin boundary condition (2). Using the numerical algorithm it is possible to observe the behavior of the optimal shape with respect to changes in the geometry of the source domain K and the changes in the value of the source g on ∂K. Numerical results show that if K is convex and $g \equiv 1$ then the optimal shape is likely to be convex. If K is non-convex it is possible to obtain non-convex optimal shapes in the case $g \equiv 1$ and also by choosing a general source term g. The results obtained with the shape optimization algorithm are in accordance with the intuition: the insulating material will concentrate in places where the value of the heat is larger. When considering constant source term, the insulator distributes uniformly around the source K, with variations depending on the shape of K and on the penalization on the area of Ω.

References

[AA09] Carlos J. S. Alves and Pedro R. S. Antunes. The method of fundamental solutions applied to the calculation of eigensolutions for 2D plates. *Internat. J. Numer. Methods Engrg.*, 77(2):177–194, 2009.

[AB+98] Emilio Acerbi, Andrea Braides, et al. Approximation of free-discontinuity problems by elliptic functionals via Gamma-convergence. 1998.

[AC81] H.W. Alt and L. Caffarelli. Existence and regularity for a minimum problem with free boundary. *J. Reine Angew. Math.*, 325:105–144, 1981.

[AF12] Pedro R. S. Antunes and Pedro Freitas. Numerical optimization of low eigenvalues of the Dirichlet and Neumann Laplacians. *J. Optim. Theory Appl.*, 154(1):235–257, 2012.

[AV10] Pedro R. S. Antunes and Svilen S. Valtchev. A meshfree numerical method for acoustic wave propagation problems in planar domains with corners and cracks. *J. Comput. Appl. Math.*, 234(9):2646–2662, 2010.

[BDM97] Andrea Braides and Gianni Dal Maso. Non-local approximation of the Mumford-Shah functional. *Calculus of Variations and Partial Differential Equations*, 5(4):293–322, 1997.

[BG15] Dorin Bucur and Alessandro Giacomini. Shape optimization problems with Robin conditions on the free boundary. In *Annales de l'Institut Henri Poincare (C) Non Linear Analysis*. Elsevier, 2015.

[BL14] Dorin Bucur and Stephan Luckhaus. Monotonicity formula and regularity for general free discontinuity problems. *Archive for Rational Mechanics and Analysis*, 211(2):489–511, 2014.

[Bog16] Beniamin Bogosel. The method of fundamental solution applied to boundary eigenvalue problems. *Journal of Computational and Applied Mathematics*, 306:265–285, 2016.

[Bra98] Andrea Braides. *Approximation of Free-Discontinuity Problems.* Lecture Notes in Mathematics, Vol. 1694, Springer-Verlag, pp. 89–91, 1998.

[CDK13] Fabien Caubet, Marc Dambrine, and Djalil Kateb. Shape optimization methods for the inverse obstacle problem with generalized impedance boundary conditions. *Inverse Problems*, 29(11):115011, 26, 2013.

[CK16] Luis A Caffarelli and Dennis Kriventsov. A free boundary problem related to thermal insulation. *Communications in Partial Differential Equations*, 41(7):1149–1182, 2016.

[DKL16] M. Dambrine, D. Kateb, and J. Lamboley. An extremal eigenvalue problem for the Wentzell-Laplace operator. *Ann. Inst. H. Poincaré Anal. Non Linéaire*, 33(2):409–450, 2016.

[GC99] M. A. Golberg and C. S. Chen. The method of fundamental solutions for potential, Helmholtz and diffusion problems. In *Boundary integral methods: numerical and mathematical aspects*, volume 1 of *Comput. Eng.*, pages 103–176. WIT Press/Comput. Mech. Publ., Boston, MA, 1999.

[Gus99] Karl E. Gustafson. *Introduction to partial differential equations and Hilbert space methods.* Dover Publications, Inc., Mineola, NY, 1999. Combined and corrected reprint of the 2nd (1987) and 3rd (1993) editions.

[Mar17] Foare Marion. *Analyse d'Images par des méthodes variationnelles et géométriques.* PhD thesis, Université de Grenoble-Alpes, 2017.

[Ost10] Braxton Osting. Optimization of spectral functions of Dirichlet-Laplacian eigenvalues. *J. Comput. Phys.*, 229(22):8578–8590, 2010.

[Sch12] Mark Schmidt. minfunc, 2012. http://www.cs.ubc.ca/ schmidtm/Software/minFunc.html.

(Beniamin Bogosel) Centre de Mathématiques Appliquées, École Polytechnique, France
E-mail address, B. Bogosel: `beniamin.bogosel@cmap.polytechnique.fr`

(Marion Foare) Laboratoire de Mathématiques, Université Savoie Mont Blanc, France
E-mail address, B. Bogosel: `marion.foare@univ-smb.fr`